



Effects of Nb doping on microstructure and photocatalytic properties of TiO₂ thin film

Min Yin, Xiaozhen Liu, Lifang Hu, Lei Xu, Jie He*

School of Chemical Engineering, Anhui University of Science and Technology, Huainan 232001, China, Tel./Fax: +86 554 6668520; emails: L_X199023@163.com (M. Yin), wangyuanlx9911@163.com (X. Liu), hlf19900223@163.com (L. Hu), 0735yinmin@163.com (L. Xu), jhe@aust.edu.cn (J. He)

Received 20 January 2014; Accepted 20 January 2015

ABSTRACT

Pure TiO₂ and Nb-doped TiO₂ thin films deposited on quartz glass substrate were prepared by the sol-gel method. The morphologies, microstructure and spectral absorption properties of the as-prepared TiO₂ thin films were investigated by scanning electron microscope (SEM), atomic force microscope (AFM) and UV-VIS absorption spectra (UV-VIS). The photocatalytic activity of the TiO₂ thin films was evaluated by the degradation of methyl orange under ultraviolet illumination. The results showed that after Nb-doping the grain size of Nb-doped TiO₂ particles was decreased to some extent and the pore size distribution was affected, but the morphology was changed negligibly. Moreover, the Nb-doping could produce a blue shift in the optical absorption edge compared to that of the pure TiO₂ thin film. The Nb-doped TiO₂ film showed lower photocatalytic activity for the degradation of methyl orange. We also investigated the effect of the number of layers on methyl orange degradation. The more the coating amount, the thicker the TiO₂ thin film and the higher photocatalytic efficiency.

Keywords: TiO₂ thin film; Nb-doping; Microstructure; Photocatalytic activity; Methyl Orange

1. Introduction

Titanium dioxide (TiO₂) is a n-type wide-bandgap oxide semiconductor material. It has been extensively investigated for various applications, such as photo-voltaic cells, dye-sensitized solar cells, batteries, optical fibres, chemical sensors, photonic crystals and photocatalysts [1–5]. Moreover, TiO₂ loaded on the surface of the porous carrier can enhance the adsorption capacity and the photocatalytic degradation efficiency of the catalyst for the material pollutants [4,5]. TiO₂ loaded on other substrates such as glass and

ceramic was expected to become self-cleaning photocatalyst due to the superhydrophilic nature [6,7].

The band gap of TiO₂ is 3.2 eV for anatase and 3.0 eV for rutile, respectively. The energy distribution of solar light is 4% UV light, 44% visible light and 52% infrared (IR) light. It is well known that the wide band gap of the TiO₂ can only absorb UV light, which largely limits the harvesting of solar light. Therefore, lots of efforts have been made to make it photocatalytic-functional in the visible wavelength regions. Some researchers modified TiO₂ through doping with transition metal, such as Fe, Mo, Nb, Sb, V, W and so on [8–14] to extend its photocatalytic application. Among these transition metals, Nb is found to be very effective in enhancing gas responses and upgrading

*Corresponding author.

photosensitivity of TiO₂ [15]. Anukunprasert et al. [16] provided convincing evidence that the addition of Nb can retard the phase transformation of TiO₂ from the anatase to rutile as well as inhibit its inner grains from growing. Lü et al. [17] reported the further enhancement of electron transport in Nb-doped TiO₂ nanoparticles via pressure-induced phase transitions. Pressure-treated Nb-doped TiO₂ with unique properties surpassing those in the anatase phase holds great promise for energy-related applications. Different types of TiO₂ such as nanotubes, nanorods, nanofibres, nanowires and nanoparticles were doped with Nb which modified its optical, electronic and magnetic properties to be used as gas sensors, solar cells, lithium ion batteries, photocatalysts and so on [18–22].

In present study, Nb-doping TiO₂ thin film deposited on the quartz glass substrate were prepared by the technology of sol-gel. The microstructure of the film was characterized by the means of scanning electron microscopy (SEM) and atomic force microscopy (AFM). The photocatalytic activity was evaluated by degradation of methyl orange. The effect of Nb⁵⁺-doping on the microstructure and photocatalytic activity of TiO₂ thin film was investigated.

2. Experimental

2.1. Material synthesis

All films were prepared by the sol-gel method. TiO₂ sol was obtained as follows: tetrabutyl titanate, ethyl alcohol and diethanolamine, which were used as precursor, solvent and stabilizer, respectively, were mixed. The mixture was stirred till a clear and transparent sol was obtained. And then, the sol was aged at 313 K for 18 h. The Nb-doped TiO₂ sol solution was prepared by the addition of niobium oxalate to the TiO₂ sol solution with the Nb/Ti mole ratio of 0.043.

The thin films were prepared with a dip-coating method. The quartz glass substrate, which had been treated by ultrasonic in distilled water was immersed in the above gel. The coating was dried at 373 K for 30 min, and then thermal treatment in air at 773 K for 2 h. The multilayer films were prepared by repeated the process of immersion, drying and calcination.

2.2. Characterization of samples

SEM images of the samples were got with field emission scanning electron micro analyser (Hitachi S-4800), employing an accelerating voltage of 10 kV. UV–VIS absorption spectra were recorded with the TU-1901 UV–VIS spectrophotometer (Beijing Purkinje General Instrument Co. Ltd.). The AFM images were

obtained on the ZL 3000 atomic force microscope (Shanghai Zhuolun MicroNano).

2.3. Photocatalytic activity testing

The photocatalytic degradation of aqueous methyl orange was carried in an evaporation pan. The TiO₂ thin film with a certain area was immersed in 100 mL aqueous methyl orange with a concentration of 15 mg L⁻¹. The pan was irradiated by 300 W ultraviolet lamp (peak wavelength = 365 nm) and the distance between the lamp and the pan is ca. 25 cm. The solution was analyzed with a UV–VIS spectrophotometer at a certain time interval.

The degradation rate of methyl orange (*D*) is calculated with the following equation:

$$D\% = \left(\frac{C_0 - C}{C_0} \right) \times 100\% = \left(\frac{A_0 - A}{A_0} \right) \times 100\%$$

where, *A*₀ is the absorbance value corresponding to concentration *C*₀, *A* is the value to *C*.

3. Results and discussion

3.1. Morphology of as-prepared samples

To gain well insight into the morphology and growth situation of pure TiO₂ thin film, the morphology and cross-sectional view of monolayer TiO₂ thin film was observed by SEM, and the results were shown in Fig. 1.

As shown in Fig. 1(a), the pure TiO₂ thin film had uniform density and crack-free structure. And it was composed of spherical-like particles and integrated tightly between the particles. Simultaneously, it can be seen that the average particle diameter of the spherical-like particles is about 40 nm. The film can be uniformly coated on the quartz glass matrix, and it presented obviously porous structure. The cross-sectional view of TiO₂ coating film (Fig. 1(b)) showed that the thickness of the film is about 0.29 μm and the film integrated tightly with the quartz glass matrix.

After Nb was doped into the pure TiO₂ thin film, the surface morphology and cross-sectional of monolayer and trilaminar Nb-doped TiO₂ coating film were shown in Figs. 2 and 3.

As shown in Figs. 2 and 3, the average diameter of the spherical-like particles decreased to 30 nm when Nb was doped into TiO₂ thin film, and the uniformity of TiO₂ thin film fell, which also can be seen from the Fig. 4. The thickness of monolayer thin film is about 0.20 μm. These results demonstrated that the lattice

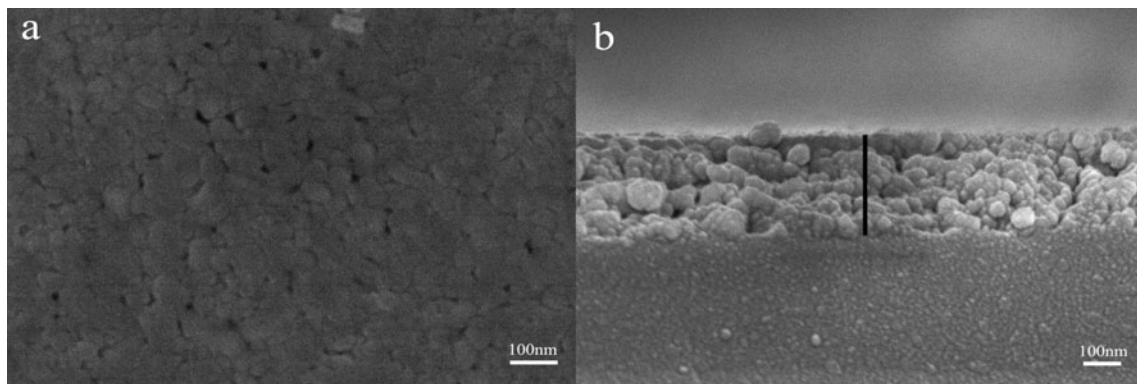


Fig. 1. Morphology (a) and cross-sectional view (b) of pure TiO_2 thin film.

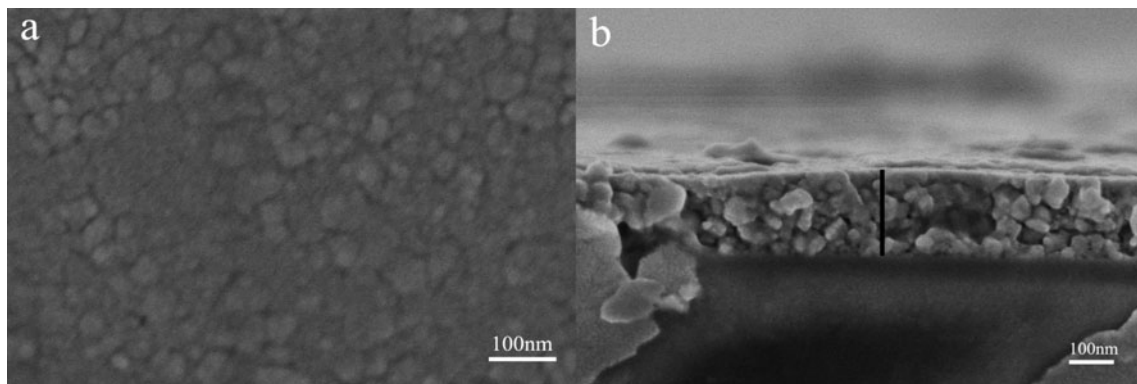


Fig. 2. Morphology (a) and cross-sectional view (b) of Nb doped TiO_2 monolayer coating film (the molar ratio of Nb:Ti is 0.043:1).

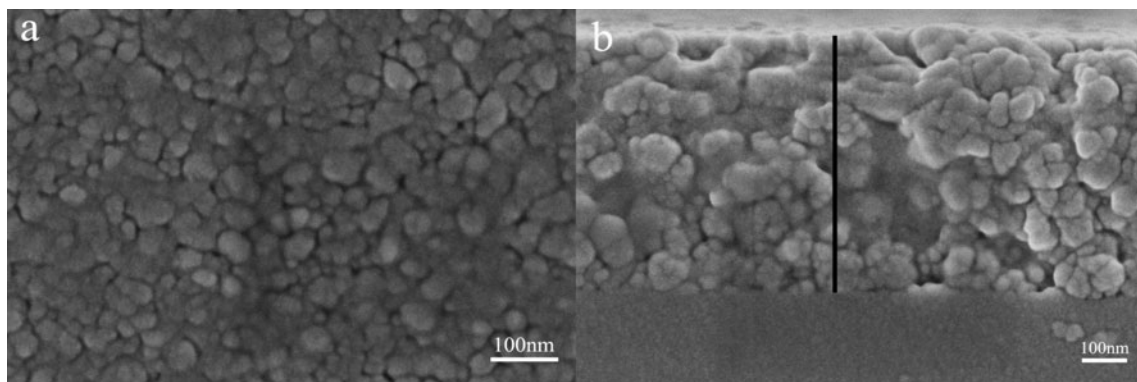


Fig. 3. Morphology (a) and cross-sectional view (b) of Nb doped TiO_2 trilaminar coating film (the molar ratio of Nb:Ti is 0.043:1).

and phase structure of TiO_2 thin film had been changed by Nb doping. Thus, the average diameter of TiO_2 microsphere and the thickness of TiO_2 monolayer thin film were decreased simultaneously.

Compared to the monolayer TiO_2 thin film, the porosity of the trilaminar TiO_2 thin film (Fig. 3) increased significantly and the pore structure brought about the increase of surface area.

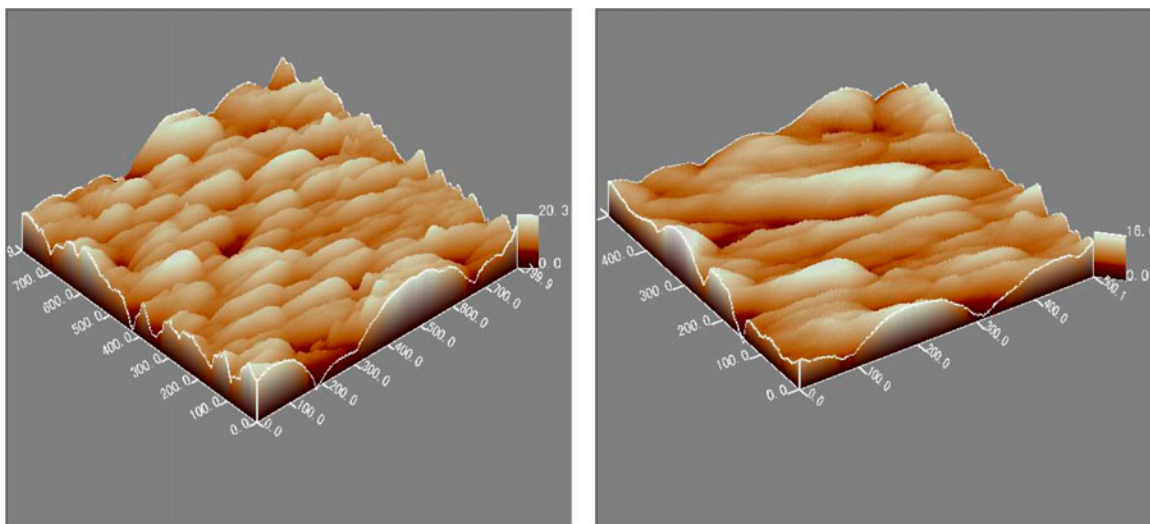


Fig. 4. AFM images of Nb-doped TiO₂ trilaminar coating film (the molar ratio of Nb:Ti is 0.043:1).

3.2. UV–VIS spectra of as-prepared samples

UV–VIS spectra of TiO₂ films with different coating layers were shown in Fig. 5.

Fig. 5 showed that TiO₂ thin films with different coating layers possessed different UV–VIS spectral responses. The absorption edge was red shifted with the increase of the coating layers. The monolayer TiO₂ thin film had larger band gap energy attribute to the quantum effect of the smaller particle size. The change of the particle size with the number of coating layers is due to the first thin film as the grain nucleus to the next film. The particle size is gradually increased with the increase of coating layers. As the result, the spectral response is shifted to long wavelength. Thus,

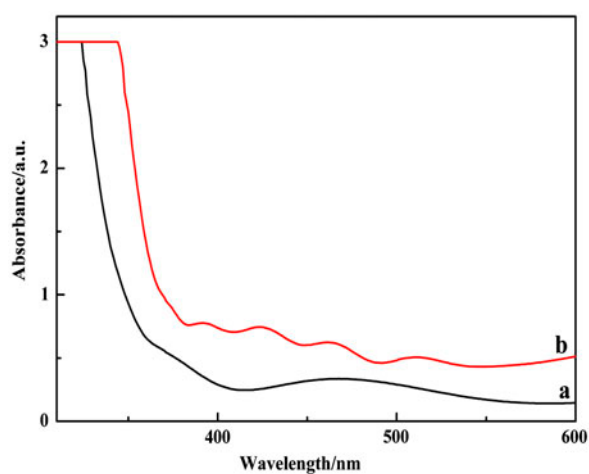


Fig. 5. UV–VIS spectra of pure TiO₂ thin films with different thickness (a) monolayer and (b) trilaminar.

the absorption spectrum of trilaminar TiO₂ thin film was shifted to a longer wavelength.

The effects of the UV–VIS spectra of Nb-doped TiO₂ thin films with different coating layers were investigated and the results were shown in Fig. 6.

Fig. 6 showed that the absorption edge of Nb-doped TiO₂ film produced blue shift in comparison to that of the pure TiO₂ film, which is ascribed to the Burstein–Moss effect [23,24]. It is known that transition metal ions can be conveniently substituted into the TiO₂ lattice, if their ionic radii were comparable to that of the Ti⁴⁺ cation [25,26]. The Nb⁵⁺ ionic radius is slightly larger than the Ti⁴⁺ ionic radius. As we mentioned in

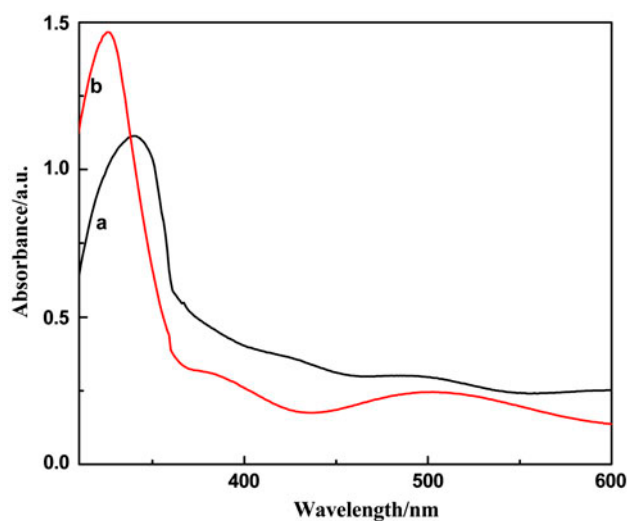


Fig. 6. The ultraviolet absorption spectra of Nb-doped TiO₂ films with different coating layers the molar ratio of Nb:Ti is 0.043:1 (a) monolayer and (b) trilaminar.

Fig. 2, the Nb^{5+} was introduced into TiO_2 lattice as a dopant, and the supplementary charge was introduced into the lattice. As the result, Ti vacancies were created, which lead to an upper shift of the conduction band edge of the Nb-doped TiO_2 thin film.

3.3. Photocatalytic performance

The degradation rates of methyl orange on pure TiO_2 and Nb-doped TiO_2 thin films with different coating layers were shown in Figs. 7 and 8.

As shown in Fig. 7, the degradation rate of methyl orange on monolayer TiO_2 film is 93% and on the trilaminar coating film is 97% under UV radiation for 4 h. It indicated that the degradation rate was improved with the increase of the pure TiO_2 thin film thickness. This is mainly attributed to the increase of the porous structure and the surface area of the trilaminar film. It is generally acknowledged that the adsorption capacity is relative to the thickness of the coating film. The thinner the thickness of TiO_2 thin film, the thinner the space charge layer. The resistance of the thin film will be larger, and directly affect the separation of the electron-hole. According to Sheng et al. [27], the photocatalytic performance was low when the thickness of the TiO_2 film reach a certain thickness, and the photocatalytic performance meaningfully enhanced when the thickness of the TiO_2 thin film reach a certain value (150–200 nm), which was due to the ultraviolet radiation had a certain depth and for the real catalytic role, film also had a certain depth in the photocatalytic reaction.

Fig. 8 showed that the degradation rate of methyl orange was improved with the increase of thickness of

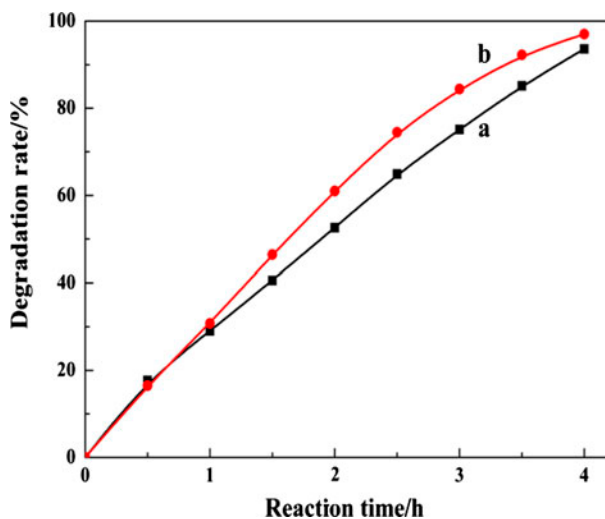


Fig. 7. The relation between coating layer and degradation rate of pure TiO_2 films (a) monolayer and (b) trilaminar.

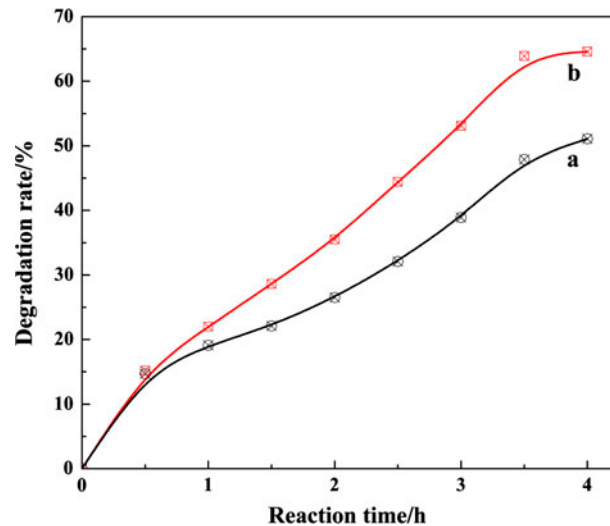


Fig. 8. The relation between coating layer and degradation rate of Nb-doped TiO_2 films (the molar ratio of Nb:Ti is 0.043:1) (a) monolayer and (b) trilaminar.

the Nb-doped TiO_2 thin film. It may be resulted from the significant increase of the porosity and surface area for the trilaminar coating film. Figs. 7 and 8 show that the photocatalytic activity of the Nb-doped TiO_2 film was lower than the pure TiO_2 film. It may be attributed to the substitutional doping with Nb^{5+} in Ti^{4+} positions and the formation of cation vacancies to maintain charge neutrality to the TiO_2 lattice. A lower photocatalytic activity is attributed to an increased hole-electron recombination rate due to the vacancy site formation in the TiO_2 lattice.

4. Conclusions

TiO_2 thin film prepared by the sol-gel method had uniform density and consistent microstructure. The film integrated tightly with the quartz glass matrix and showed obvious porous structure in the film. The particle size of TiO_2 microsphere decreased to some extent and the uniformity was affected after Nb-doped TiO_2 thin film, the photocatalytic activity decreased significantly. The degradation rate of methyl orange was increased with the increase of the thickness of pure or Nb-doped TiO_2 thin film.

Acknowledgements

This work was supported by the Natural Science Foundation of China (No. 21271008) and Research Fund of Key Laboratory for Advanced Technology in Environmental Protection of Jiangsu Province (No. AE201106).

References

- [1] M.H. Habibi, R. Kamrani, Photocatalytic mineralization of methylene blue from water by a heterogeneous copper-titania nanocomposite film, *Desalin. Water Treat.* 46 (2012) 278–284.
- [2] P.R. Ettireddy, D. Lev, S. Panagiotis, TiO₂-loaded zeolites and mesoporous materials in the sonophotocatalytic decomposition of aqueous organic pollutants: The role of the support, *Appl. Catal., B* 42 (2003) 1–11.
- [3] J.C. Colmenares, M.A. Aramendía, A. Marinas, J.M. Marinas, F.J. Urbano, Synthesis, characterization and photocatalytic activity of different metal-doped titania systems, *Appl. Catal., A* 306 (2006) 120–127.
- [4] A. Mills, G. Hilla, S. Bhopala, I.P. Parkin, S.A. O'Neill, Thick titanium dioxide films for semiconductor photocatalysis, *J. Photochem. Photobiol., A* 160 (2003) 185–194.
- [5] Y. Zhang, J. Li, J. Wang, Substrate-assisted crystallization and photocatalytic properties of mesoporous TiO₂ thin films, *Chem. Mater.* 18 (2006) 2917–2923.
- [6] A. Mattsson, M. Leideborg, K. Larsson, G. Westin, L. Osterlund, Adsorption and solar light decomposition of acetone on anatase TiO₂ and niobium doped TiO₂ thin films, *J. Phys. Chem. B* 110 (2006) 1210–1220.
- [7] J.D. Zhuang, W.X. Dai, Q.F. Tian, Z.H. Li, L.Y. Xie, J.X. Wang, P. Liu, Photocatalytic degradation of RhB over TiO₂ bilayer films: Effect of defects and their location, *Langmuir* 26 (2010) 9686–9694.
- [8] I. Parkin, R.G. Palgrave, Self-cleaning coatings, *J. Mater. Chem.* 15 (2005) 1689–1695.
- [9] A. Kuback, G. Colon, M. Fernandez-Garcia, Cationic (V, Mo, Nb, W) doping of TiO₂-anatase: A real alternative for visible light-driven photocatalysts, *Catal. Today* 143 (2009) 286–292.
- [10] R. Subasri, M. Murugan, K. Murugan, J. Revathi, G.V.N. Rao, T.N. Rao, Investigations on the photocatalytic activity of sol-gel derived plain and Fe³⁺/Nb⁵⁺-doped titania coatings on glass substrates, *Mater. Chem. Phys.* 124 (2010) 63–68.
- [11] T. Hitosugi, A. Ueda, S. Nakao, N. Yamada, Y. Furubayashi, Y. Hirose, S. Konuma, T. Shimada, T. Hasegawa, Transparent conducting properties of anatase Ti_{0.94}Nb_{0.06}O₂ polycrystalline films on glass substrate, *Thin Solid Films* 516 (2008) 5750–5753.
- [12] C.M. Maghanga, G.A. Niklasson, C.G. Granqvist, Optical properties of sputter deposited transparent and conducting TiO₂: Nb films, *Thin Solid Films* 518 (2009) 1254–1258.
- [13] K.H. Hung, P.W. Lee, W.C. Hsu, H.C. Hsing, H.T. Chang, M.S. Wong, Transparent conducting oxide films of heavily Nb-doped titania by reactive co-sputtering, *J. Alloys Compd.* 509 (2011) 10190–10194.
- [14] L. Zhao, X.R. Zhao, J.M. Liu, A. Zhang, D.H. Wang, B.B. Wei, Fabrications of Nb-doped TiO₂ (TNO) transparent conductive oxide polycrystalline films on glass substrates by sol-gel method, *J. Sol-Gel Sci. Technol.* 53 (2010) 475–479.
- [15] M.C. Carotta, M. Ferroni, D. Gnani, V. Guidi, M. Merli, G. Martinelli, M.C. Casale, M. Notaro, Nanostructured pure and Nb-doped TiO₂ as thick film gas sensors for environmental monitoring, *Sens. Actuators, B* 58 (1999) 310–317.
- [16] T. Anukunprasert, C. Saiwan, E. Traversa, The development of gas sensor for carbon monoxide monitoring using nanostructure of Nb-TiO₂, *Sci. Technol. Adv. Mater.* 6 (2005) 359–363.
- [17] X.J. Lü, W.G. Yang, Z.W. Quan, T.Q. Lin, L.G. Bai, L. Wang, F.Q. Huang, Y.S. Zhao, Enhanced electron transport in Nb-doped TiO₂ nanoparticles via pressure-induced phase transitions, *J. Am. Chem. Soc.* 136 (2014) 419–426.
- [18] Y. Alivov, V. Singh, Y. Ding, L.J. Cerkovnik, P. Nagpal, Doping of wide-bandgap titanium-dioxide nanotubes: Optical, electronic and magnetic properties, *Nanoscale* 18 (2014) 10839–10849.
- [19] S. Singh, H. Kaur, V.N. Singh, K. Jain, T.D. Senguttuvan, Highly sensitive and pulse-like response toward ethanol of Nb doped TiO₂ nanorods based gas sensors, *Sens. Actuators, B* 171–172 (2012) 899–906.
- [20] Y. Horie, M. Deguchi, S. Guo, K. Aoki, T. Nomiya, Coating effect of electrospun nanofibers of Nb-doped TiO₂ mixed in photoelectrode of dye sensitized solar cells, *JPN. J. Appl. Phys.* 53 (2014) 05FB01: 1–6.
- [21] B. Liu, H.M. Chen, C. Liu, S.C. Andrews, C. Hahn, P.D. Yang, Large-scale synthesis of transition-metal doped TiO₂ nanowires with controllable overpotential, *J. Am. Chem. Soc.* 135 (2013) 9995–9998.
- [22] M.Q. Gao, Y.L. Xu, Y. Bai, S.H. Jin, Synthesis and characterization of Nb, F-codoped titania nanoparticles for dye-sensitized solar cells, *J. Mater. Res.* 29 (2014) 230–238.
- [23] B.E. Anomalous, Optical absorption limit in InSb, *Phys. Rev.* 93 (1954) 632–633.
- [24] T.S. Moss, The interpretation of the properties of indium antimonide, *Proc. Phys. Soc. London, Sect. A* 67 (1954) 775–782.
- [25] A.K. Chandiran, F. Sauvage, M. Casas-Cabanas, P. Comte, S.M. Zakeeruddin, M. Graetzel, Doping a TiO₂ photoanode with Nb⁵⁺ to enhance transparency and charge collection efficiency in dye-sensitized solar cells, *J. Phys. Chem. C* 114 (2010) 15849–15856.
- [26] C.N. Zhang, S.H. Chen, L. Mo, Y. Huang, H.J. Tian, L.H. Hu, Z.P. Huo, S.Y. Dai, F.T. Kong, X. Pan, Charge recombination and band-edge shift in the dye-sensitized Mg²⁺-doped TiO₂ solar cells, *J. Phys. Chem. C* 115 (2011) 16418–16424.
- [27] J. Sheng, L. Shivalingappa, J. Karasawa, T. Fukami, Preparation and photocatalysis evaluation of anatase film on Pt-buffered polyimide, *Vacuum* 51 (1998) 623–627.